Adsorption (2009) 15: 278–286
DOI 10.1007/s10450-009-9175-8

Synthesis, structure and adsorption properties of nanoporous SBA-15 materials with framework and surface functionalities

M. Barczak · S. Pikus · Barbara Skrzydło-Radomańska · A. Dąbrowski

Published online: 10 April 2009

Abstract Highly ordered SBA-15 nanoporous silica containing ethylene, phenylene bridges or/and amine, thiol, vinyl and phenyl surface groups were synthesized by using amphiphilic block copolymer as the structure-directing agent. The XRD data shows high degree of the order of the final structures. Obtained materials have well-developed porous structure—values of specific surface area are in the range 700–1050 m^2/g and the sizes of cylindrical mesopores are in the range 6.5–9.5 nm. It was determined that size of the mesopores strongly depends even on small amounts of co-monomers co-condensing with TEOS. A new technique to introduce some amount of pendant amine groups by co-condensation of proper monomers has been proposed. Tetragonal structure was obtained when small amount of vinyl groups was introduced to the system. A new approach of determining pore size based only on the XRD measurements was compared with KJS method, confirming full usefulness of the former for calculation of the size of mesopores in SBA-15 materials.

Keywords Adsorption · Functionalization · Sol-gel method · Hybrid materials · Ordered mesoporous materials · Nanoporous materials · Porosity · SBA-15 · XRD

Dedicated to Professor Mietek Jaroniec on the occasion of his 60th birthday.

M. Barczak (✉) · S. Pikus · A. Dąbrowski
Faculty of Chemistry, Maria Curie-Sklodowska University, Maria Curie-Sklodowska Sq. 3, 20-031 Lublin, Poland
e-mail: mbarczak@poczta.umcs.lublin.pl

B. Skrzydło-Radomańska
Department of Gastroenterology, Medical University of Lublin, Jaczewskiego 8, 20-954 Lublin, Poland

1 Introduction

Nowadays, ordered mesoporous organosilicas constitute a very exciting field in materials chemistry and have numerous potential applications due to their high surface areas, large pore volumes of ordered mesopores and narrow pore size distributions as well as the diversity of the functional groups which they can contain. Those make them especially attractive materials in catalysis, sensing, separation and adsorption application. During last fifteen years a significant progress has been achieved in the field of nanoporous molecular sieves after discovery of ordered mesoporous silicas (OMSs). Initially OMS materials were synthesized via self-assembly process driven by electrostatic interactions between the anionic silica species and cationic alkyltrimethylammonium surfactants possessing from eight to twenty two carbon atoms in the alkyl chain used as structure directing agents. Materials such as MCM-41 or FSM-16 focused a lot of attention because of their range of pore sizes beyond those achievable in zeolites (Kresge et al. 1992; Beck et al. 1992). However their pore sizes were limited to 7 nm and thin walls make them hydrothermally unstable. This put a lot of efforts to find new materials with better properties. In the 1998 novel ordered materials were obtained by replacing surfactants with amphiphilic block copolymers used as structure-directing agents (Zhao et al. 1998a, 1998b; Goltner et al. 1998). Especially, the SBA-15 materials have become one of the most popular ordered silica nanomaterials for several reasons: large mesopores (up to 15 nm), thicker pore walls, presence of irregular interconnecting micropores and high thermal and hydrothermal stabilities caused by its thicker mesopores walls (Grudzien et al. 2006a; Yang et al. 1999; Zhang et al. 2005). SBA-15 materials are usually synthesized under strong acidic conditions by employing amphiphilic triblock copolymer

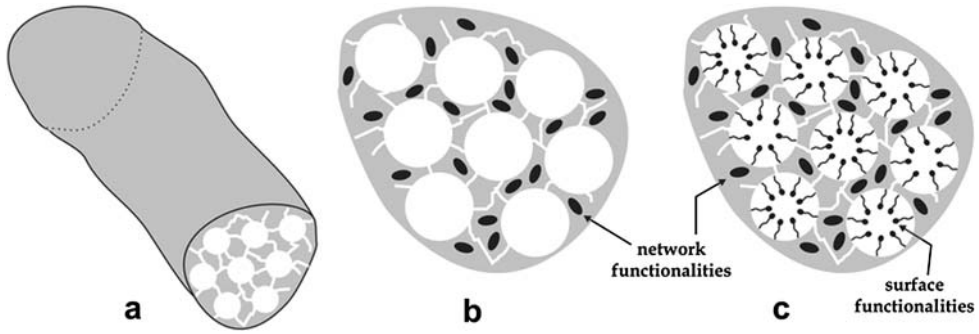

Fig. 1 (**a**) Schematic illustration of nanoporous channel-like SBA-15 structure with cylindrical mesoporous channels interconnected each other by a network of micropores and smaller mesopores, (**b**) network-functionalized SBA-15 structure (samples **6–8**, see Sect. 2), (**c**) network- and surface-functionalized SBA-15 structure (samples **3–5**, see Sect. 2)

Pluronic P123 via controlled hydrolysis and condensation of tetraethoxysilane (TEOS) followed by removal of polymeric template by either extraction with ethanol and acid or calcination at elevated temperatures. Possibility of introduction of different functional groups into the framework or the surface of OMS, makes these materials very attractive for catalytic and adsorption processes, sensing devices and environmental applications (Antochshuk et al. 2003; Andersson et al. 2004; Olkhovyk et al. 2004; Rosenholm et al. 2004; Gierszal et al. 2005; Olkhovyk and Jaroniec 2005). Such hybrid materials are known as ordered mesoporous organosilicas (OMOs). There are two main approaches for the surface functionalization: post-synthesis grafting (Feng et al. 1997; Jaroniec et al. 1998; Antochshuk and Jaroniec 1999; Zapilko and Anwander 2006) by attaching desired groups to the surface of template-free OMS, and co-condensation of silica precursor and organotrialkoxysilane in the presence of structure-directing agents (Inagaki et al. 1999; Melde et al. 1999; Gong et al. 2001; Wang et al. 2003; Wang et al. 2005; Hodgkins et al. 2005; Fiorilli et al. 2005; Grudzien et al. 2006b, 2006c; Jaroniec 2006). Such a surface functionalization leads to materials differing in the reactivity, pore accessibility and distribution of organic groups (Grudzien et al. 2006a). Particularly, the co-condensation route seems to be very attractive as it affords to control simultaneously the surface and structural properties of the resulting OMOs, even those with high loadings of pendent organic functionalities. These groups can be attached to the internal and external surfaces of mesopores as well as can be incorporated in the framework as uniformly integrated bridges. Using co-condensation route different types OMO materials have been obtained. They can contain different pendant groups like, for example, alkyl (Kruk et al. 2002), vinyl (Wang et al. 2003; Kao et al. 2006; Wei et al. 2007), carboxylic (Yang et al. 2004; Fiorilli et al. 2005), thiol (Crudden et al. 2005; Hodgkins et al. 2005; Wang et al. 2005) amine (Zhang et al. 2005; Wang et al. 2005; Maria Chong and Zhao 2003).

Co-condensation of bridged silsesquioxanes $(RO)_3Si\text{-}R\text{-}Si(OR)_3$ instead of trialkoxyorganosilane $(RO)_3Si\text{-}R$ (where R is a functional group) leads to functionalization of SBA-15 framework by organic bridging groups distributed inside the mesopore walls (Asefa et al. 1999; Inagaki et al. 2002; Melde et al. 1999; Olhovyk et al. 2005; Grudzien et al. 2006b, 2006c). The resulting materials are known as periodic mesoporous organosilicas (PMOs). This approach has been used to incorporate a variety of bridging moieties like, for example, aliphatic groups (Bao et al. 2004; Zhao et al. 2004; Liang et al. 2005), aromatic spacers such as phenylene (Inagaki et al. 2002) or thiophene (Corriu et al. 2002). Schematic picture presenting incorporation of the functional groups inside mesopore walls and in the skeleton is drawn in the Fig. 1.

Herein, we report the synthesis channel-like mesoporous organosilicas synthesized by co-condensation of tetraethoxysilane (TEOS) with bridged polysilsesquioxane monomers bearing ethylene and phenylene bridges and alkoxysilanes bearing aminopropyl, mercaptopropyl, vinyl and phenyl groups which can form surface species. Obtained materials were characterized by powder X-ray diffraction (XRD), nitrogen sorption measurements, elemental analysis and atomic force microscopy (AFM).

2 Experimental

2.1 Reagents

The following compounds were used: tetraethoxysilane (**TEOS**, 96%, ABCR), 1,2-bis(triethoxysilylethane (**BTESE**, 96%, ABCR), 1,4-bis(triethoxy-silyl)benzene (**BTESB**, 95%, Aldrich); 3-aminopropyltriethoxysilane (**APTES**, 98%, ABCR), 3-mercaptopropyltriethoxysilane (**MPTES**, 95%, ABCR), vinyltriethosysilane (**VTES**, 98%, ABCR), phenyltriethoxysilane (**PTES**, 98%, ABCR), poly(ethylene oxide)-block-poly(propylene oxide)-block-poly(ethylene oxide) triblock copolymer ($EO_{20}PO_{70}EO_{20}$, Pluronic P123, **P123**, BASF), hydrochloric acid (37%,

Table 1 XRD-derived characteristics of the materials studied

No.	Molar ratio of monomers	Symmetry	k[a]	a[b]	d/a	d[c]	w[d]
1	TEOS	hexagonal	0.36	12.3	0.66	8.1	4.2
2	TEOS/BTESE/APTES 18:1:1	–	–	–	–	–	–
3	TEOS/BTESE/MPTES 18:1:1	hexagonal	0.52	11.4	0.67	7.8	3.6
4	TEOS/BTESB/APTES 18:1:1	hexagonal	0.96	12.0	0.65	8.6	3.4
5	TEOS/BTESB/MPTES 18:1:1	hexagonal	0.35	10.0	0.65	6.5	3.5
6	TEOS/PTES 18:2	hexagonal	0.08	11.4	0.62	7.1	4.3
7	TEOS/VTES 18:2	tetragonal	–	9.3 21.3	–	–	–
8	TEOS/PTES/VTES 18:1:1	tetragonal	–	9.0 21.1	–	–	–

[a] k = ratio of the intensity of the signals I_{110} and I_{200}, $k = I_{110}/I_{200}$

[b] Unit cell parameter (in the case of the samples **7** and **8**, two unit cell parameters are given, **a** and **c**, respectively) (nm)

[c] Size of the pores (nm) (see (Barrett et al. 1951)

[d] Pore wall thickness (nm)

POCH), ethanol (99.8%, POCH). Deionized water (DW; resistivity <17.5 MΩ cm) was obtained using Millipore ion-exchange purification system. All chemicals were used as received without further purification.

2.2 Syntheses of the samples

Syntheses of all channel-like mesoporous SBA-15 silicas were performed in the presence of P123 triblock copolymer by co-condensation of TEOS and organotrialkoxysilane (APTES, MPTES, VTES or PTES) or/and bridged silsesquioxane (BTESE or BTESB) to introduce the desired surface and framework functional groups. All functionalized SBA-15 materials were synthesized by one-pot route using by the similar synthesis procedure reported elsewhere (Grudzien et al. 2006d). In a model synthesis, 2 g of P123 was dissolved in 61 ml of 2 M HCl and 11 ml of deionized water under vigorous stirring at 40 °C. After 6 h of stirring a specified volume of TEOS was added dropwise to this solution under vigorous mixing, and then after 15 minutes proper co-monomer was pipetted to achieve the desired molar composition of both silanes. Numeration of the samples and initial molar composition of monomers used to their synthesis is given in Table 1.

In the case of samples **2–5**, the bridged organobis(triethoxysilane) (BTESE or BTESB) was pipetted after 10 minutes, and the organotriethoxysilane (APTES or MPTES) after next 5 minutes. The resulting mixture was stirred for 24 h and aged at 100 °C for 48 h. The white solids were thoroughly washed with deionized water, filtered and dried at 70 °C.

The template was removed by triple extraction with the acidic absolute ethanol (99.8%) at 70 °C. TG measurements (not described here) confirm that this extraction procedure turned to be effective for the removal of almost all the template from the samples. Loss of mass in the range of 200–700 °C indicates that in the final samples there is no more than 1.5% of Pluronic P123.

2.3 Measurements

Powder X-ray diffraction (XRD) patterns were recorded using a Seifert RTG DRON-3 diffractometer (CuKα radiation) with 0.02° step size and 10 s step time over a range $0.5° < 2\theta < 5.0°$ at room temperature.

Nitrogen adsorption isotherms were measured at −196 °C by using an ASAP 2405N adsorption analyzer (Micromeritics). Prior to adsorption measurements each sample was degassed (at 110 °C). The BET surface area (S_{BET}) was evaluated in the 0.05–0.25 range of relative pressures (Brunauer et al. 1938). The total pore volume (V_p) was calculated by converting the amount adsorbed at a relative pressure about 0.99 to the volume of liquid adsorbate. The average pore size (d) was estimated using the BJH (Barrett et al. 1951) and KJS method (Kruk et al. 1997). Pore size distributions were estimated using the same approach.

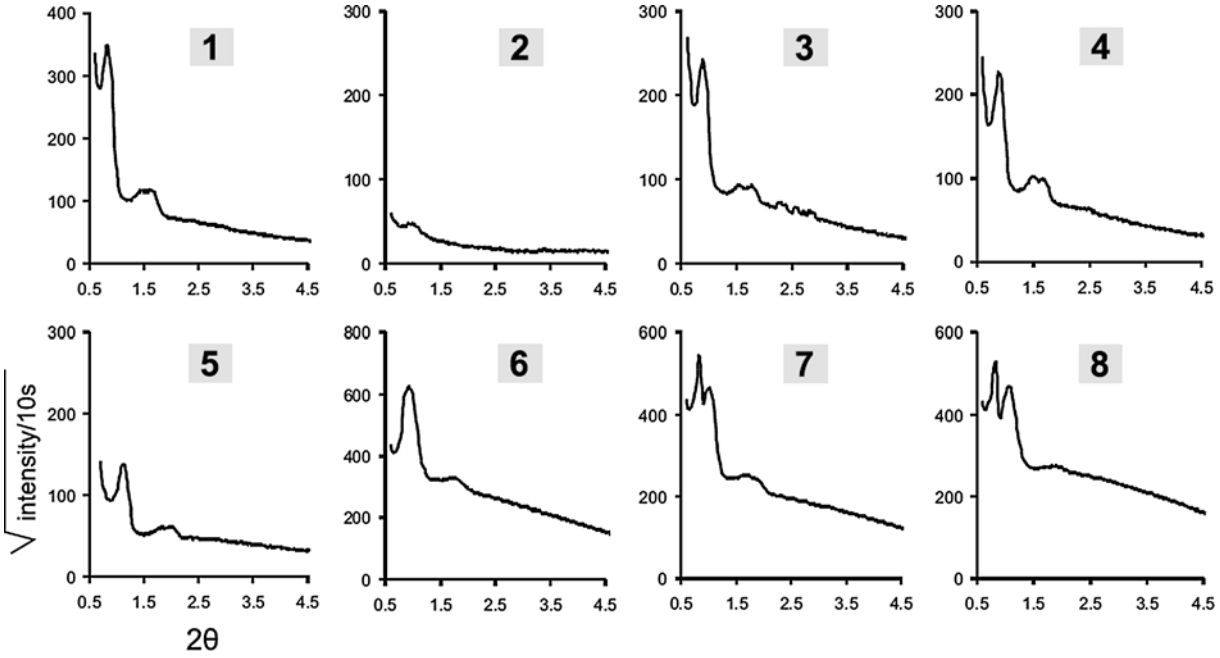

Fig. 2 XRD patterns of the samples studied

The content of the amine in the obtained samples was determined quantitatively by elemental analysis using Perkin-Elmer CHN 2400 analyzator and the content of the thiol groups by X-ray fluorescence spectroscopy (XRF) using the Canberra Apparatus.

AFM images were received using MultiMode Scanning Probe Microscope "Nanoscope III" (Digital Instruments). The imaging technique was TappingMode and the scan size was 500 nm.

3 Results and discussion

3.1 XRD

Figure 2 presents the XRD patterns for the samples **1–8**. Under all conditions investigated, mesostructured materials, albeit with different degree of order, were obtained, apart only one exception: the totally disordered sample **2**—reason for such a behavior will be explained in the text. Three well-resolved peaks in the case of samples **1**, **3–6** are observed in the range of $2\theta \approx 0.8$–$2°$. The peaks can be indexed according to two-dimensional hexagonal *p6mm* symmetry, indicating a well-defined SBA-15 mesostructure: one sharp reflection at $2\theta \approx 0.8$ indexed as (100) and two minor but distinct reflections at $2\theta \approx 1.5$ and $2\theta \approx 2$, indexed as (110) and (200), respectively. Only the sample **2** has totally disordered structure which is confirmed by the lack of diffraction peaks on corresponding XRD pattern. The unit cell parameters for the samples studied are presented in Table 1.

Samples **2** and **4** attract special attention because of completely different type of their structure ordering despite the fact that both were synthesized in the same conditions. The only difference in the synthesis' procedure was the type of network-functionalizing monomer used: BTESE or BTESB for samples **2** and **4**, respectively (see Table 1). Thus, the only factor potentially affecting the final structure is the presence of phenylene spacer, and more precisely π-electrons. Surface functionalization with amine groups performed according to the synthesis' procedure but without the presence of BTESB leads to a disordered product. It is believed that a reason for such a behavior is connected with interactions between amine groups and poly(ethylene oxide) blocks so the SBA-15 ordering is much more sensitive to amine groups than to other functionalities. A strong disruptive effect of APTES on the formation of an ordered structure was described elsewhere where very low concentration of APTES (APTES/TEOS = 1:20) resulted in a material with only one very broad XRD peak (Chong et al. 2004). In order to improve the mesoscopical order of amine-functionalized SBA-15 the non-simultaneous adding of the monomers during the synthesis allowing TEOS to prehydrolyze was proposed. Such a procedure was previously described in the literature (Wang et al. 2005). However in the case of sample **4** even simultaneous adding of the monomers resulted in highly-ordered SBA-15 material. A reason of such a phenomenon could be explained as follows. In strongly acidic condition of synthesis all amine groups are protonated. Without presence of benzene rings these protonated groups strongly interact with ethylene chains of the triblock copolymer affecting the micelle

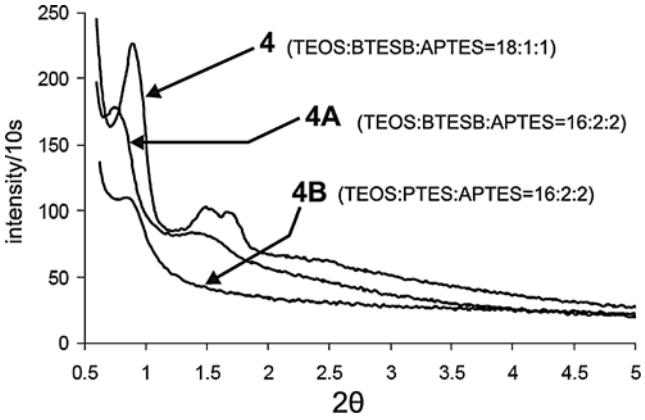

Fig. 3 The comparison of XRD patterns for samples synthesized with increasing amount of APTES (sample *4* vs. *4A*) and replacing BTESB by PTES (sample *4A* vs. *4B*)

formation leading to destroying the ordered structure of the final material. When the benzene rings are present, the protonated amine groups preferably interact much stronger with the π-electrons rather than with ethylene chains not affecting the ordered structure. As a result the material obtained is highly-ordered.

However, our attempts to introduce higher content of amine groups were unsuccessful and the deterioration of mesostructural ordering was observed—see Fig. 3. On the XRD pattern of the sample **4A** synthesized from the mixture of monomers in the ratio: TEOS/BTESB/APTES = 16:2:2 lack of separation of the (110) and (200) reflections and a decrease of the intensity of the (100) signal comparing with sample **4** is observed. Replacing one of the monomers (BTESB) by another (PTES) in the initial mixture of monomers (sample **4B**) leads to total disordering of the structure and no reflections on XRD patterns are observed.

Up to now in the case of APTES-functionalized SBA-15 materials by simultaneous co-condensation it is very difficult, or sometimes impossible, to see three peaks, namely 100, 110 and 200. Normally only one very broad peak at $2\theta \approx 1^\circ$ is observed. One of the approaches is to extend the time interval between addition of TEOS and APTES to several hours. Such a strategy was successfully employed to obtain OMOs with high degree of order. In this case well-ordered samples are obtained due to the fact that pure-silica precursor is able to form temporary rigid network before amine groups destroy the ordering.

Sample **4** was obtained by simultaneous addition of all monomers; total time interval when all three monomers had been added was only 15 minutes. It shows that the co-condensation proposed in this paper (with the use of BTESB as one of co-monomers) can be applied to the synthesis of amine-functionalized OMOs.

Interesting results have been obtained for samples **7** and **8** which were synthesized by co-condensation of TEOS with VTES (sample **7**) and TEOS with VTES and PTES (sample **8**). Additional intensive peaks on the XRD patterns are observed for these samples in comparison to the rest of the samples. As for the hexagonally ordered samples with *p6mm* symmetry only one peak is always observed at $2\theta \approx 1$, the change of the XRD pattern testifies to different type of symmetry of the samples **7** and **8**. It was described earlier that higher concentration of VTES during the synthesis lead to materials with *Ia3d* symmetry (Wang et al. 2003). However, amount of VTES used by us to synthesize samples **7** and **8** (see Table 1) was much lower than that used in the work (Wang et al. 2003). Obtained structure can not be indexed as cubic or hexagonal system, however, it complies with high accuracy the rules of tetragonal system. Thus, the peaks on the XRD patterns of samples **7** and **8** have been indexed as 002, 101, 004, 104, respectively, what allowed to obtain the following values of unit cell parameters: sample 7 ($a = 9.288$ nm, $c = 21.32$ nm), sample 8 ($a = 9.012$ nm, $c = 21.12$ nm).

From the results it is evident, that small amount of VTES used to co-condense with TEOS changed the type of the structure. The symmetry of the resulted samples is apparently different than this obtained when higher concentration of VTES is used in the initial mixture with TEOS (Wang et al. 2003).

3.2 Nitrogen adsorption

Nitrogen adsorption/desorption isotherms of the materials studied are shown in Fig. 4. All samples exhibit type IV adsorption-desorption isotherms. Isotherms of the samples **1**,**3–6** have a sharp capillary condensation step, reflecting capillary condensation of adsorbate in the uniform mesopores channels, and evaporation step related to the evacuation of adsorbate from the pores. Thus, it can be concluded that a framework of materials **1**,**3–6** has a rather uniform array of mesopores with the same diameter, what is also supported by XRD patterns (Fig. 2). Samples **7** and **8** have a less sharp capillary condensation step, what testifies to deterioration of the structure's ordering. Totally different shape of the isotherm is observed for sample **2** what testifies to absence of ordered array of mesopores; in fact this sample is totally amorphous.

The parameters of the porous structure are summarized in Table 2. All materials exhibit high values of surface area (S_{BET}) ranging from 700 to 1050 m^2/g. Pure silica sample **1** has the lowest S_{BET} value—700 m^2/g, samples **2–5** has S_{BET} values the range 780–840 m^2/g. The highest values of S_{BET} are observed in the case of the vinyl and vinyl/phenyl functionalized samples **7–8**: 970–1060 m^2/g (what additionally confirms that for these samples a new type of structure was formed). Pore volumes (V_p) also differ among the samples investigated. Relatively high pore

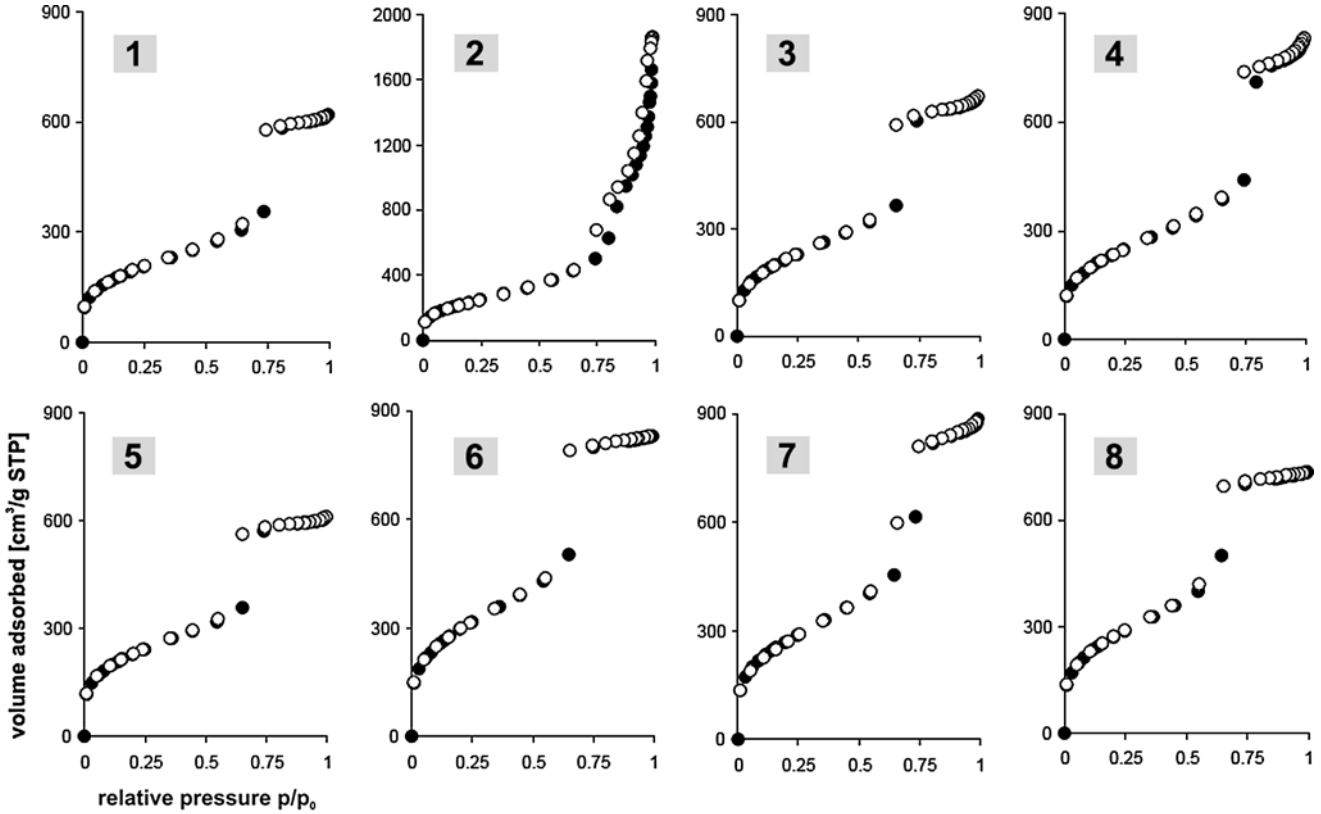

Fig. 4 Nitrogen adsorption/desorption isotherms of the samples studied

Table 2 Structure-adsorption characteristics of the materials studied

No.	Molar ratio of monomers	S_{BET} (m^2/g)	V_p (cm^3/g)	d_{BJH} (nm)	d_{KJS} (nm)	d_{XRD} (nm)
1	TEOS	700	0.95	5.6	9.3	8.1
2	TEOS/BTESE/APTES 18:1:1	842	2.31	11.4	–	–
3	TEOS/BTESE/MPTES 18:1:1	777	1.02	4.6	7.7	7.8
4	TEOS/BTESB/APTES 18:1:1	836	1.26	5.7	9.2	8.6
5	TEOS/BTESB/MPTES 18:1:1	820	0.93	4.3	7.7	6.5
6	TEOS/PTES 18:2	1063	1.28	4.8	8.2	7.1
7	TEOS/VTES 18:2	973	1.35	5.4	7.9	–
8	TEOS/PTES/VTES 18:1:1	976	1.13	4.6	8.0	–

volume of the sample **2** is a result of the lack of order and a presence of textural unordered mesopores. The rest of the samples have pore volumes in the range 0.93–1.35 cm^3/g.

Pore sizes of the samples **1–8** were calculated using BJH (Barrett et al. 1951) and KJS (Kruk et al. 1997) method (d_{BJH} and d_{KJS}, respectively), which are commonly used to calculate pore size distributions of SBA-15 materials.

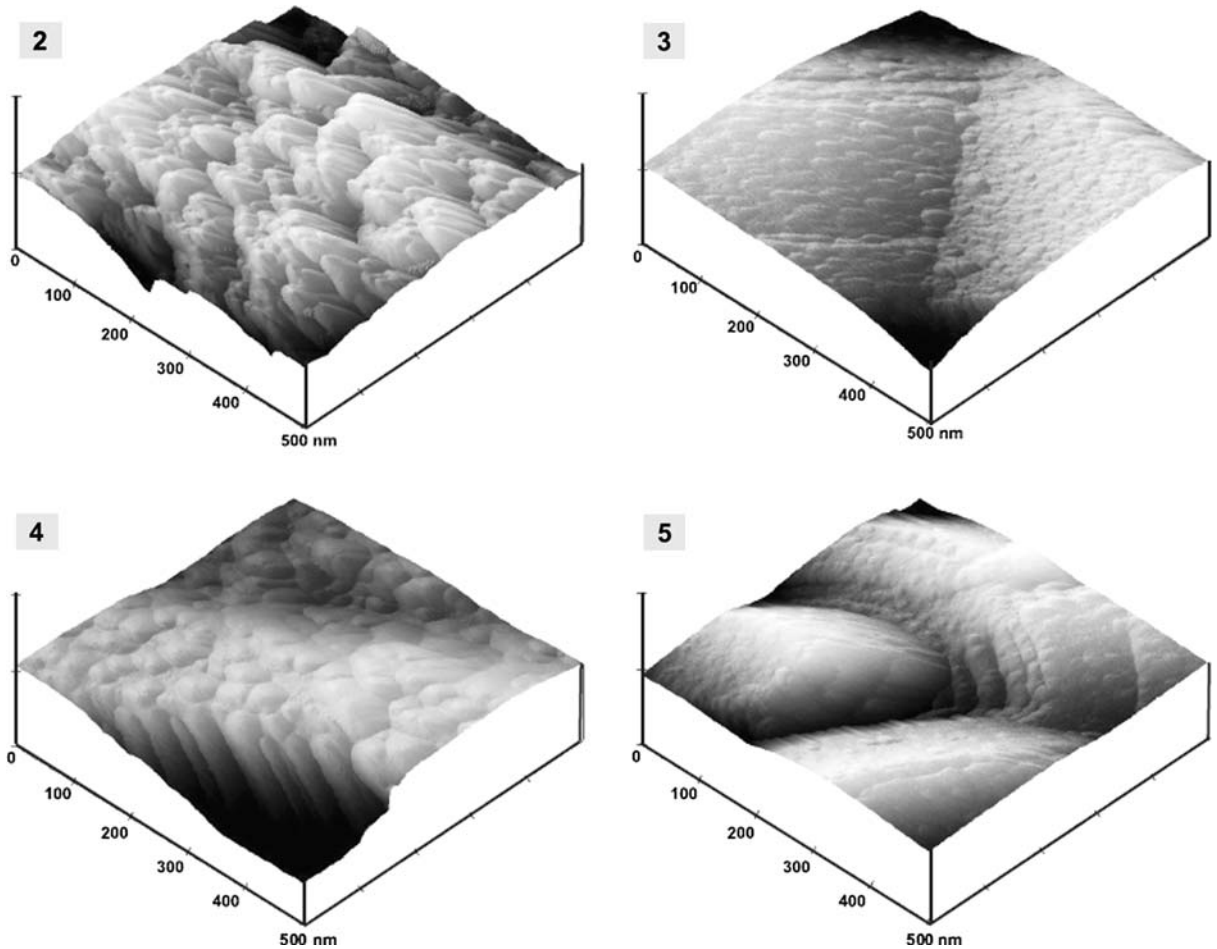

Fig. 5 AFM images of the samples **2–5**

However, the BJH method tends to underestimate the average pore size, so usually the KJS method is recommended for more accurate calculations. It should be underlined that a very good agreement between the KJS method and the method proposed recently by Pikus et al. (2007) is observed. This makes the latter an appropriate tool to calculate average mesopores size of SBA-15 materials, independently from adsorption data. Average pore sizes of primary mesopores of all ordered samples calculated by KJS method are in the range 7.7–9.3 nm. The smallest pore sizes are observed in the case of thiol-functionalized organosilicas, independently on the type of the bridge present in the framework (ethylene vs phenylene)—7.7 nm. Both, pure silica sample **1** and amine functionalized sample **5** have the biggest average mesopore size: 9.3 and 9.2 nm, respectively.

3.3 Atomic Force Microscopy

AFM images of the samples **2–5** are presented in Fig. 5. The images show differences in the samples' surface structure. These synthesized with the use of APTES (samples **2** and **4**) are less regular than those obtained when MPTES was used as a co-monomer (samples **3** and **5**). It can be also seen that difference in the ordering of sample **2** and **4** has his reflection in the AFM images of these samples: the surface of the former is clearly less regular that the surface of the latter.

3.4 Presence of the amine and thiol groups

The nitrogen and sulfur contents for the samples **2–5** obtained by elemental analysis represent around 40–75% of the values estimated on the basis of the initial molar composition of the synthesis mixture, indicating quite good efficiency of incorporation of above-mentioned functionalities. This efficiency was higher in the case of thiol groups (60–75%) than in the case of amine groups (40–55%). Apparently, some part of the amine groups is lost during the extraction process. The content of phenyl and vinyl functionalities in the samples **6–8** was difficult to estimate due to the presence of some small amount of unextracted template in the final samples.

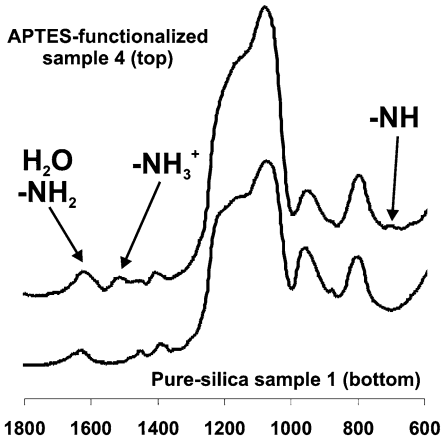

Fig. 6 Fragments of the FT-IR spectra of the samples **1** and **4**

The incorporation of amine groups in the silicate network can be qualitatively confirmed by FT-IR spectroscopy. A week peak is seen in the case of sample **4** at ∼705 cm^{-1} due to the bending of N–H bonds (Wang et al. 2005; Maria Chong and Zhao 2003). The medium-intensity peak attributed to the $–NH_3^+$ bending at ∼1515 cm^{-1} also indicates the existence of amine groups (Wang et al. 2005; Maria Chong and Zhao 2003). An increase in the intensity of the absorption band at ∼1635 cm^{-1} (which probably correspond not only to $\delta(H_2O)$ but also to $\delta(NH_2)$) seems to be some indication of the presence of the amine groups (Maria Chong and Zhao 2003). It should be mentioned that two absorption bands corresponding to the stretching NH modes, $\nu^{s,as}(NH)$, normally located in the region of ∼3300–3500 cm^{-1}, cannot be observed due to the presence of a wide band of the physically adsorbed water.

The presence of thiol groups in the samples **3** and **5** could not be detected by means of FT-IR/PAS spectroscopy due to low concentration of MTES used in the synthesis. However, we were able to detect the thiol groups by means of Raman spectroscopy, where the presence of the band at 2580 cm^{-1}, attributed to SH stretching mode, $\nu(SH)$, is a clear evidence of the successful co-condensation between TEOS and MPTES.

4 Conclusions

Mesoporous SBA-15 organosilicas with surface amine and thiol groups were prepared by direct co-condensation of appropriate monomers. Both, structural parameters (S_{BET}, V_p, d) and degree of ordering are dependent upon the type of functionalized silane used in the synthesis. It was shown that simultaneous addition of certain amount of amine groups leads to ordered structure if the phenylene bridge monomer is also present in the initial mixture. However, the higher concentrations of amine groups make the final sample less ordered or even unordered, which is reflected by disappearance of the diffraction peaks on XRD patterns.

In the case of vinyl and vinyl/phenyl functionalized SBA-15 organosilicas the type of ordering is rather tetragonal than hexagonal testifying to the fact that even relatively small amount of co-monomer added during the synthesis can affect the final structure and type of ordering.

Two methods of determining the average mesopores size, KJS method (Brunauer et al. 1938) and method based only on the XRD measurements (Barrett et al. 1951), has been tested showing a good convergence between these two.

Acknowledgements A. Dabrowski and M. Barczak thank the Polish Ministry of Higher Education and Science for supporting this research under Grant No. N N204 111135.

References

Andersson, J., Rosenholm, J., Areva, S., Linden, M., Chem. Mater. **16**, 4160 (2004)
Antochshuk, V., Jaroniec, M.: J. Phys. Chem. B **103**, 6252 (1999)
Antochshuk, V., Olkhovyk, O., Jaroniec, M., Park, I.-S., Ryoo, R.: Langmuir **19**, 3031 (2003)
Asefa, T., MacLachlan, M.J., Coombos, N., Ozin, G.A.: Nature **402**, 867 (1999)
Bao, X.Y., Zhao, X.S., Li, X., Chia, P.A., Li, J.: J. Phys. Chem. B **108**, 4684 (2004)
Barrett, E.P., Joyner, L.G., Halenda, P.: J. Am. Chem. Soc. **73**, 373 (1951)
Beck, S., et al.: J. Am. Chem. Soc. **114**, 10834 (1992)
Brunauer, J.S., Emmet, P.H., Teller, E.: J. Am. Chem. Soc. **60**, 309 (1938)
Chong, A.S., Zhao, X.S., Kustedjo, A.T., Qiao, S.Z.: Microporous Mesoporous Mater. **72**, 33 (2004)
Corriu, R.J.P., Mehdi, A., Reye, C., Thieulux, C.: Chem. Commun. 1382 (2002)
Crudden, C.M., Sateesh, M., Lewis, R.: J. Am. Chem. Soc. **9**(127), 28 (2005)
Feng, X., Fryxell, G.E., Wang, L.Q., Kim, A.Y., Liu, J., Kemmer, K.: Science **276**, 923 (1997)
Fiorilli, S., Ondia, B., Bonelli, B., Garrone, E.: J. Phys. Chem. B **109**, 16725 (2005)
Gierszal, K.P., Kim, T.-W., Ryoo, R., Jaroniec, M.: J. Phys. Chem. B **109**, 23263 (2005)
Goltner, C.G., Henke, S., Weissenberger, M.C., Antonietti, M.: Angew. Chem. Int. Ed. **37**, 613 (1998)
Gong, Y.J., Li, Z.H., Wu, D., Sun, Y.H., Deng, F., Luo, Q., Yue, Y.: Microporous Mesoporous Mater. **49**, 95 (2001)
Grudzien, R.M., Grabicka, B.E., Knobloch, D.J., Jaroniec, M.: Coll. & Surf. A: Physicochem. Eng. Aspects **291**, 139 (2006a)
Grudzien, R.M., Pikus, S., Jaroniec, M.: J. Phys. Chem. B **110**, 2972 (2006b)
Grudzien, R.M., Grabicka, B.E., Pikus, S., Jaroniec, M.: Chem. Mater. **18**, 1722 (2006c)
Grudzien, R.M., Grabicka, B.E., Jaroniec, M.: Adsorption **12**, 293 (2006d)
Hodgkins, R.P., Garcia-Bennett, A.E., Wright, P.A.: Microporous Mesoporous Mater. **79**, 241–252 (2005)
Inagaki, S., Guan, S., Fukushima, Y., Ohsuna, T., Teresaki, O.: J. Am. Chem. Soc. **121**, 9611 (1999)
Inagaki, S., Guan, S., Ohsuna, T., Teraski, O.: Nature **416**, 204 (2002)

Jaroniec, C.P., Kruk, M., Jaroniec, M., Sayari, A.: J. Phys. Chem. B **102**, 5503 (1998)
Jaroniec, M.: Nature **442**, 638 (2006)
Kao, H.M., Wu, J.-D., Cheng, Ch.-Ch., Chiang, A.S.T.: Microporous Mesoporous Mater. **88**, 319 (2006)
Kresge, C.T., Leonowicz, M.E., Roth, W.J., Vartuli, J.C., Beck, J.S.: Nature **359**, 710 (1992)
Kruk, M., Jaroniec, M., Sayari, A.: Langmuir **13**, 6267 (1997)
Kruk, M., Asefa, T., Coombs, N., Jaroniec, M., Ozin, A.G.: J. Mater. Chem. **12**, 3452 (2002)
Liang, Y., Hanzlik, M., Anwander, R.: J. Mater. Chem. **15**, 3919 (2005)
Maria Chong, A.S., Zhao, X.S.: J. Phys. Chem. B **107**, 12650–12657 (2003)
Melde, B.J., Holland, B.T., Blandford, C.F., Stein, A.: Chem. Mater. **11**, 3302 (1999)
Olhovyk, O., Pikus, S., Jaroniec, M.: J. Mater. Chem. **15**, 1517 (2005)
Olkhovyk, O., Antochshuk, V., Jaroniec, M.: Coll. Surf. A **236**, 69 (2004)
Olkhovyk, O., Jaroniec, M.: Adsorption **11**, 205 (2005)
Pikus, S., Solovyov, L.A., Kozak, M., Jaroniec, M.: Appl. Surf. Sci. **253**, 5682 (2007)
Rosenholm, J.B., Rahiala, H., Puputti, J., Stathopolous, V., Pomonis, P., Beurroies, I., Backfolk, K.: Coll. Surf. A **250**, 289 (2004)
Wang, Y.Q., Yang, C.M., Zibrowius, B., Spliethoff, B., Linden, M., Schuth, F.: Chem. Mater. **15**, 5029 (2003)
Wang, X., Lin, K.S.K., Chan, J.C.C., Cheng, S.: J. Phys. B **109**, 1763 (2005)
Wang, X., Lin, K.S.K., Chan, J.C.C., Cheng, S.: J. Phys. B **109**, 1763 (2005)
Wei, Q., et al.: Mater. Let. **61**, 1469–1473 (2007)
Yang, P., Zhao, D., Margolese, D.I., Chmelka, B.F., Stucky, G.D.: Chem. Mater. **11**, 2813 (1999)
Yang, C.-M., Wang, Y., Zibrowius, B., Schuth, F.: Phys. Chem. Chem. Phys. **6**, 2461 (2004)
Zapilko, C., Anwander, R.: Chem. Mater. **18**, 1479 (2006)
Zhang, F., Yan, Y., Yang, H., Meng, Y., Yu, Ch., Tu, B., Zhao, D.: J. Phys. Chem. B **109**, 8273 (2005)
Zhao, L., Zhu, G., Zhang, D., Di, Y., Teresaki, O., Qiu, Sh.: J. Phys. Chem. B **109**, 764 (2004)
Zhao, D., Feng, J., Huo, Q., Melosh, N., Fredrickson, G.H., Chmelka, B.F., Stucky, G.D.: Science **279**, 548 (1998a)
Zhao, D., Huo, Q., Feng, J., Chmelka, B.F., Stucky, G.D.: J. Am. Chem. Soc. **120**, 6024 (1998b)